Intravitreal Stanniocalcin-1 Enhances New Blood Vessel Growth in a Rat Model of Laser-Induced Choroidal Neovascularization

Min Zhao,[1,2] Wankun Xie,[1,2] Shu-Huai Tsai,[2] Travis W. Hein,[1,2] Brent A. Rocke,[3] Lih Kuo,[1,2] and Robert H. Rosa Jr[1,2]

[1]Ophthalmic Vascular Research Program, Department of Ophthalmology, Scott & White Eye Institute, Temple, Texas, United States
[2]Department of Medical Physiology, Texas A&M University Health Science Center, Temple, Texas, United States
[3]Olin E. Teague Veterans' Medical Center, Central Texas Veterans Health Care System, Temple, Texas, United States

Correspondence: Robert H. Rosa Jr, Scott & White Eye Institute, 1815 South 31st Street, Temple, TX 76504, USA;
robert.rosa@bswhealth.org.
Lih Kuo, Texas A&M HSC, 702 SW HK Dodgen Loop, Temple, TX 76504, USA;
lkuo@tamhsc.edu.

LK and RHR contributed equally to the work presented here and should therefore be regarded as equivalent authors.

PURPOSE. The purpose of this study was to investigate the impact of stanniocalcin-1 (STC-1), a photoreceptor-protective glycoprotein, on the development of choroidal neovascularization (CNV) in relation to VEGF and its main receptor (VEGFR2) expression after laser injury.

METHODS. In rats, CNV was induced by laser photocoagulation in both eyes, followed by intravitreal injection of STC-1 in the right eye and vehicle or denatured STC-1 injection in the left eye as control. Two weeks after laser injury, fundus autofluorescence (FAF) imaging and fundus fluorescein angiography (FFA) were performed. Fluorescein leakage from CNV was graded using a defined scale system. The size of CNV was quantified with spectral domain optical coherence tomography (SD-OCT), fluorescein-labeled choroid-sclera flat mounts, and hematoxylin-eosin staining. Protein expressions were evaluated by Western blot.

RESULTS. Photocoagulation produced a well-circumscribed area of CNV. With STC-1 treatment, CNV lesions assessed by FAF were increased by 50% in both intensity and area. The CNV lesions were also increased with SD-OCT, flat-mount, and histologic analyses. FFA disclosed enhanced fluorescein leakage in CNV lesions in STC-1 treated eyes. The STC-1 protein was detected in the choroidal tissue and its level was increased with CNV lesions in correlation with VEGF and VEGFR2 expressions. Intravitreal administration of STC-1 significantly increased choroidal expression of both VEGF and VEGFR2 proteins.

CONCLUSIONS. Chorodial tissue expresses STC-1, which seemingly acts as a stress response protein by enhancing pathological new blood vessel growth in laser-induced CNV. It is likely that STC-1 promotes CNV development via VEGF signaling.

Keywords: optical coherence tomography, fundus autofluorescence, vascular endothelial growth factor, vascular endothelial growth factor receptor 2

Stanniocalcin-1 (STC-1) is a secreted glycoprotein initially discovered in bony fish as a calcium-reducing factor for calcium-phosphate regulation in the fish gill.[1,2] STC-1 is also expressed in human tissues and organs, including the kidney, heart, liver, lung, prostate, adrenal gland, and ovary.[3–5] Although previous studies have suggested various roles for STC-1 in developmental and pathophysiological processes,[6–8] including promotion of carcinogenesis[9–11] and modulation of angiogenesis,[7,11–14] the impact of STC-1 on ocular pathophysiology remains unclear.

AMD is one of the leading causes of irreversible vision loss in the elderly and is associated with various genetic and environmental risk factors, including oxidative stress, inflammation, and an imbalance in pro- and anti-angiogenic factors.[15–18] AMD is generally classified into two subtypes, dry or nonexudative AMD and wet or exudative AMD. Oxidative stress and photoreceptor apoptosis are prominent features of dry AMD, whereas choroidal neovascularization (CNV) is the pathologic hallmark of wet AMD.[19–21] Neovascularization is a complex process mediated by a wide array of growth factor families and protease enzymes, such as VEGF, FGF, matrix metalloproteinase, angiopoietin, and possibly STC proteins.[14,22,23] These angiogenic factors may stimulate and/or modulate endothelial cell proliferation, migration, and maturation.

We previously demonstrated that STC-1 can protect retinal morphology and function by reducing oxidative stress and photoreceptor apoptosis in four rodent models of inherited retinal degeneration.[24,25] Interestingly, the STC-1 gene was found to be highly upregulated in the vasculature of colon carcinomas.[26] Subsequently, its roles in modulating endothelial cell migration and morphogenesis were suggested in an in vitro cell culture study.[13] In the mouse ischemic hindlimb, STC-1 expression was found to increase in parallel with endothelial cell marker CD31, suggesting possible involvement of STC-1 in modulating pathological angiogenesis.[13] Although a recent in vitro study demonstrated that STC-1 can promote proliferation, migration, and tube formation of cultured human umbilical vein endothelial cells (HUVECs) likely through VEGF signaling,[14] the impact of STC-1 in pathological ocular neovascularization and its relationship with VEGF and its main receptor VEGFR2 in vivo remains unclear. Herein, we studied the effect of STC-1 on

the expression of VEGF and VEGFR2 in the development of CNV induced by laser injury in the rat eye. The CNV lesions were assessed with fundus imaging of autofluorescence and fluorescein angiography, spectral domain optical coherence tomography (SD-OCT), choroid-sclera flat mounts, and histology.

MATERIALS AND METHODS

Animal Use and Welfare

Animal experiments were performed following the ARVO Statement for the Use of Animals in Ophthalmic and Vision Research and were approved by the Institutional Animal Care and Use Committee of Scott & White Medical Center. Brown-Norway Rats (180–200 g, 6–8 weeks) were obtained from Charles River Laboratories (Charleston, SC, USA).

CNV Induction by Laser Photocoagulation

Animals were anesthetized with intraperitoneal injections of 50 mg/kg ketamine and 10 mg/kg xylazine, and the pupil was dilated with topical application of 0.5% tropicamide (Alcon, Ft. Worth, TX, USA). After lubricating the cornea with GenTeal Gel (Novartis, Basel, Switzerland), photocoagulation was performed using a 532-nm wavelength laser and a slit lamp (NIDEK, Fremont, CA, USA). The laser burn (50 μm, 200 mW, 0.1 s) was generated between each main retinal vessel approximately two disc diameters from the optic nerve head. Each eye received a total of four to six laser burns. Bubbles on the retina created by the laser light indicated the success of laser injury due to rupture of Bruch membrane. Lesions with hemorrhage or without bubbles were excluded from further study. Animals were euthanized by CO_2 inhalation 2 weeks after laser photocoagulation. Rats without laser treatment were used as normal controls for comparison. Immediately after laser photocoagulation, all animals received an intravitreal injection of human recombinant STC-1 (5 μL, 0.5 μg/μL; BioVendor, Asheville, NC, USA) in the right eye and balanced salt solution (BSS, 5 μL; Alcon) or denatured STC-1 (5 μL, 0.5 μg/μL) in the left eye as control using a 32-gauge Hamilton syringe (Hamilton, Reno, NV, USA). Heat denatured STC-1 protein was prepared by heating the protein solution at 99°C for 60 minutes. Topical anesthesia was applied with 0.5% proparacaine (Akorn, Lake Forest, IL, USA) followed by topical Betadine 5% Sterile Ophthalmic Prep Solution (Alcon) before the injection. TobraDex ophthalmic ointment (Alcon) was applied immediately after the injection to reduce postinjection inflammation and the risk of infection.

Fundus Autofluorescence (FAF), SD-OCT, and In Vivo Measurement of CNV Volume

FAF and SD-OCT were performed using the Heidelberg Spectralis HRA+OCT (Heidelberg, Germany). The pupils were dilated with topical tropicamide (0.5%; Alcon) and the cornea was lubricated with GenTeal Gel (Novartis) before examination. The outlines of the CNV lesions in FAF images were manually selected, and the area and intensity of autofluorescence were analyzed using ImageJ software (http://imagej.nih.gov/ij/; provided in the public domain by the National Institutes of Health, Bethesda, MD, USA). For each CNV lesion, SD-OCT high-resolution horizontal and vertical scanning images were taken to calculate the volume of the CNV lesion as previously described.[27] The CNV lesion was defined as a spindle-shaped hyperreflective area at the level of the RPE.

Only the scan that passed through the center of the lesion was chosen for the evaluation of the width, thickness, and length of the lesion. CNV volume was quantified using Heidelberg Engineering software (Heidelberg Eye Explorer) based on the ellipsoid volume formula,[27] $V = (4/3) \pi (a \cdot b \cdot c)$, where a, b, and c are three elliptic radii. The elliptic axes of the ellipsoid, $2a$, $2b$, and $2c$, represent the CNV width, length, and thickness, respectively.

Fundus Fluorescein Angiography (FFA)

FFA was performed using the Heidelberg Spectralis HRA+OCT. Early-phase and late-phase FFA images were recorded at 1 to 5 minutes and 15 to 25 minutes, respectively, after intraperitoneal injection of fluorescein sodium (10%, 0.3 mL; Alcon). Leakage was defined as the presence of an early hyperfluorescent spot that increased in size and/or intensity with time in late-phase angiography.[28] The grade of leakage was assigned as described previously[29,30]: 0, "no leakage," faint hyperfluorescence or mottled fluorescence; 1, "questionable leakage," hyperfluorescent lesion without progressive increase in size or intensity; 2, "leaky," hyperfluorescence increasing in intensity but not in size; 3, "pathologically significant leakage," hyperfluorescence increasing in both intensity and size. Late-phase images were chosen for analysis of fluorescein leakage to correspond with the clearance time of fluorescein from the vasculature and to avoid interference with the observation of hyperfluorescence from CNV.[31] FFA was graded by two masked investigators. When the two grades for a lesion did not match, the two investigators discussed the lesion grades and agreed on the final grade together.

RPE-Choroid-Sclera Flat Mounts, Immunofluorescence, and Ex Vivo CNV Measurements

High-molecular-weight FITC-dextran (molecular weight 2×10^6 g/mol; Sigma-Aldrich, St. Louis, MO, USA) was administered through intracardiac injection (5 mL, 50 mg/mL) under anesthesia. Animals were then euthanized by CO_2 inhalation. Eyes were enucleated and fixed in 4% paraformaldehyde for 30 minutes. The anterior segment and lens were removed, and the retina was separated from the remaining posterior segment (RPE-choroid-sclera) with fine curved forceps and scissors. The RPE-choroid-sclera complex was cut radially into four petals and then flat-mounted onto a slide and covered with a coverslip.[32] Some of the eye cups were incubated with primary antibody against STC-1 (sc-30183; Santa Cruz, Dallas, TX, USA) overnight at 4°C and then washed and incubated with the Cy3-conjugated secondary antibody for 3 hours and finally washed and incubated with 4,6-diamidino-2-phenylindole (DAPI) for 5 minutes at room temperature.[33] The RPE-choroid-sclera complex was cut radially into four petals and then flat-mounted onto a slide and covered with a coverslip. The flat-mount images were obtained with a fluorescence microscope (Axiovert 200M; Carl Zeiss Microscopy GmbH, Oberkochen, Germany). Lesion area was manually measured with the Carl Zeiss image solution software (AxioVision; Carl Zeiss Microscopy GmbH).

Histological Analysis of CNV

Eyes were enucleated, fixed in 4% formaldehyde, and then embedded in paraffin. The samples were serially sectioned and stained with hematoxylin-eosin. The section that passed through the center of each lesion with the largest cross-sectional area was chosen to evaluate the area of the CNV lesion. Images were obtained with an Olympus microscope
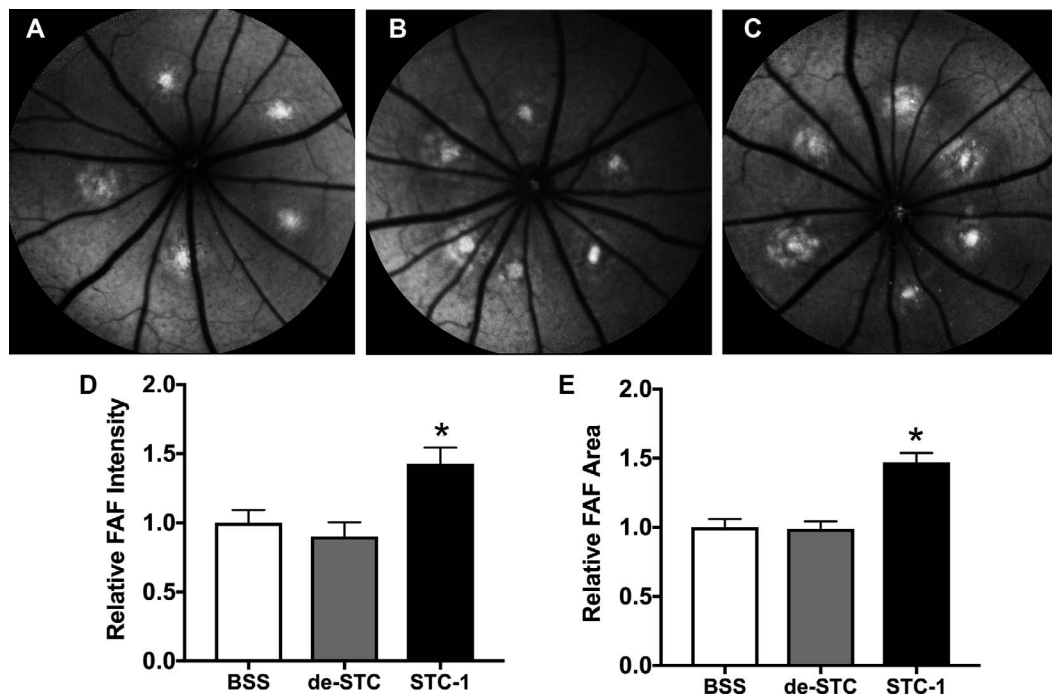
FIGURE 1. FAF imaging of laser-induced CNV. FAF images (**A–C**) were obtained 2 weeks after laser photocoagulation. Representative FAF images of the control group (**A**, laser-induced CNV + intravitreal BSS; $n = 7$ animals), denatured STC-1 (de-STC) treatment group (**B**, laser-induced CNV + intravitreal de-STC; $n = 3$ animals), and STC-1 treatment group (**C**; laser-induced CNV + intravitreal STC-1; $n = 7$ animals) are shown. The intensity of FAF (**D**) was significantly increased in the STC-1 treatment group (*$P < 0.05$ vs. BSS and de-STC; 1-way ANOVA followed by Tukey's test). The area of FAF (**E**) was significantly increased in the STC-1 treatment group (*$P < 0.05$ vs. BSS and de-STC; 1-way ANOVA followed by Tukey's test). The area and intensity of FAF were not different between BSS and de-STC groups (**D**, **E**).

(IX81; Olympus, Tokyo, Japan), and the CNV lesion area was analyzed with the Olympus image analysis software (cell-Sens).

Western Blot Analysis

RPE/choroidal tissues were isolated from eyecups and then lysed in Tissue Extraction Reagent I buffer (Invitrogen, Carlsbad, CA, USA) containing protease inhibitor cocktail according to the manufacturer's instructions. Total protein concentration was determined by bicinchoninic acid protein assay (Pierce Biotechnology, Rockford, IL, USA). The same amount of protein (10 μg) was loaded in 4% to 15% precast polyacrylamide Tris-HCL gels (Bio-Rad, Hercules, CA, USA). After electrophoresis, proteins were transferred to a nitrocellulose membrane (Bio-Rad) and then blocked with 5% skim milk for 1 hour. The membrane was incubated with primary antibody against VEGF (sc-507; Santa Cruz), VEGFR2 (#9698; Cell Signaling, Danvers, MA, USA), STC-1 (sc-30183; Santa Cruz), and β-actin (#4970; Cell Signaling) overnight at 4°C, and then washed and incubated with horseradish peroxidase–conjugated secondary antibody for 1 hour at room temperature. Proteins of interest were detected with enhanced chemilumescent reagents (Pierce Biotechnology) and the ratios of VEGF, VEGFR2, and STC-1 expressions to β-actin expression were determined. These values from the treatment groups were normalized to the average of the normal control group and expressed as a relative ratio for comparison.

Statistics

The average CNV volume and FAF intensity and area were calculated from four to six lesions in each eye as a single datum point from one animal, and six to eight animals were used for each series of experiments. A total of 70 eyes were studied, and 6 eyes were excluded from data analysis due to vitreous hemorrhage, lack of hyperfluorescence in the lesion, or merging of adjacent lesions. The CNV measurement data from STC-1 and denatured STC-1 treatments were normalized to the average of the BSS group for comparison. The data are expressed as mean ± SEM. Statistical analysis was performed using Student's *t*-test, 1-way ANOVA, followed by Tukey's multiple comparisons test, or χ^2 test when appropriate. *P* values <0.05 were considered statistically significant.

RESULTS

FAF Imaging of Laser-induced CNV

Two weeks after laser injury, the retinal fundus lesions exhibited a small, well-circumscribed area of increased FAF centrally surrounded by a ring of decreased FAF in BSS (Fig. 1A), denatured STC-1 (Fig. 1B), and STC-1 (Fig. 1C) -treated eyes. Both intensity (Fig. 1D) and area (Fig. 1E) of the FAF in the CNV lesion were significantly increased by 50% in the eyes treated with STC-1 compared with eyes treated with BSS or denatured STC-1 control. There was no significant difference between the denatured STC-1 group and the BSS group in both intensity and area of FAF.

FFA and Leakage Grade of Laser-induced CNV

Two weeks after laser injury, the CNV lesion was assessed by grading fluorescein leakage. Compared with the BSS-treated groups (Fig. 2A), there was no difference in fluorescein leakage in the eyes treated with denatured STC-1 (Fig. 2B). On the other hand, FFA disclosed increased fluorescein leakage from
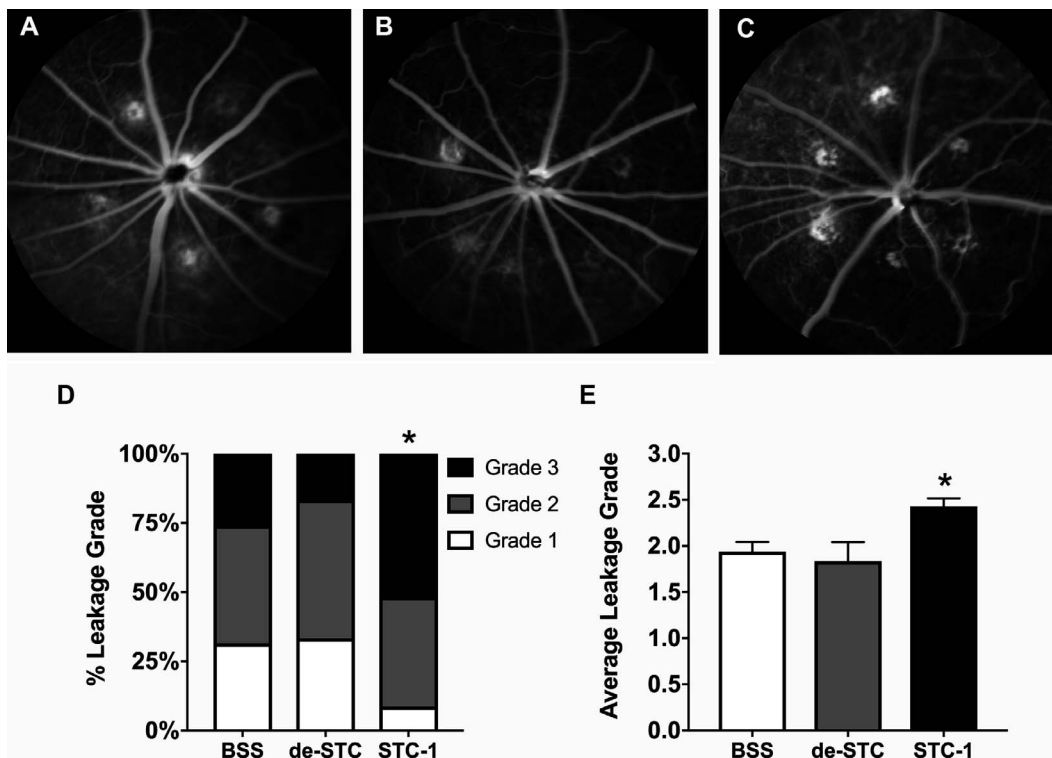
FIGURE 2. FFA of laser-induced CNV. FFA was performed 2 weeks after laser photocoagulation (A–C). Representative FFA images of the control group (A, laser-induced CNV + intravitreal BSS), de-STC treatment group (B, laser-induced CNV + intravitreal de-STC), and STC-1 treatment group (C, laser-induced CNV + intravitreal STC-1) are shown. The distribution and proportion of the lesion leakage grades were not altered by administration of de-STC ($n = 3$ animals) compared with BSS treatment ($n = 9$ animals), but they were significantly altered by STC-1 ($n = 9$ animals) administration (D, *$P < 0.05$ vs. BSS and de-STC; χ^2 test). There was no difference in the average leakage grade between BSS (1.9 ± 0.2) and de-STC (1.8 ± 0.2) groups, but STC-1 treatment increased the average leakage grade (2.4 ± 0.1) (E, *$P < 0.05$ vs. BSS and de-STC; 1-way ANOVA followed by Tukey's test).

CNV lesions after STC-1 treatment (Fig. 2C). The distribution and proportion of the lesion grades with BSS treatment were not different from those with denatured STC-1 treatment (Fig. 2D); however, STC-1 treatment significantly increased the grade 3 fluorescein leakage from approximately 25% (BSS treatment) to approximately 52% of all CNV lesions (Fig. 2D). On average, the leakage grade was significantly higher in STC-1–treated eyes (2.4 ± 0.1) compared with BSS-treated eyes (1.9 ± 0.1) (Fig. 2E). In eyes treated with denatured STC-1, grade 3 fluorescein leakage represented approximately 17% of all CNV lesions (Fig. 2D), and the average leakage grade (1.8 ± 0.2) was not significantly different from that of BSS-treated eyes (1.9 ± 0.1) (Fig. 2E).

CNV Volume Assessed With SD-OCT

The CNV lesions appeared as spindle-shaped, hyperreflective areas on SD-OCT (Figs. 3A, 3B). Horizontal (Fig. 3C) and vertical (Fig. 3D) high-resolution SD-OCT scans were obtained through the central aspect of the CNV lesions. From these scans, the greatest linear diameter in two dimensions (2a and 2b) and the height of the CNV lesions (2c) were used to calculate the CNV volume, where a, b, and c are three elliptic radii (Fig. 3E). Compared with BSS-treated control eyes (Fig. 3A), the CNV lesion size was increased in the eyes treated with STC-1 (Fig. 3B). On average, the CNV volume was increased approximately 50% in the eyes treated with STC-1 (Fig. 3F). No significant difference in the CNV lesion size was observed by SD-OCT between eyes treated with denatured STC-1 and BSS (Fig. 3F).

RPE-Choroid-Sclera Flat Mounts and Histology of CNV

On flat-mount preparations, the laser-induced CNV lesions appeared as well-circumscribed, spoke-wheel–shaped complexes in BSS-treated eyes (Fig. 4A). Serial histologic sections through the CNV lesions disclosed a rupture in Bruch membrane with loss of the photoreceptors and RPE centrally, and fusiform fibrovascular tissue with vascular endothelium, scattered pigmented cells (including RPE and/or pigment-laden macrophages), fibroblasts, and new collagen in the BSS-treated eyes (Fig. 4B, Supplementary Fig. S1A). Focal retinal gliosis was present centrally with pigment migration into the retina overlying the CNV lesions. In the peripheral aspect of the CNV lesion, the photoreceptors were disorganized with variable attenuation and hypertrophy of the RPE (Fig. 4B, Supplementary Fig. S1A). The size of the CNV lesion assessed with RPE-choroid-sclera flat mounts (Fig. 4C) or histology (Fig. 4D) was increased in the eyes treated with STC-1. Quantitative analysis showed approximately 75% and approximately 30% increase in the CNV lesion area by STC-1 in the flat-mount preparation (Fig. 4E) and hematoxylin-eosin staining (Fig. 4F), respectively.

STC-1 Expression in RPE/Choroidal Tissue

STC-1 protein expression was detected in RPE/choroidal tissue of normal eyes (Fig. 5A), and its expression level was significantly elevated in the RPE/choroidal tissue 2 weeks after laser photocoagulation (Fig. 5B). Immunofluorescence signal of STC-1 was detected in the CNV lesion and in normal-
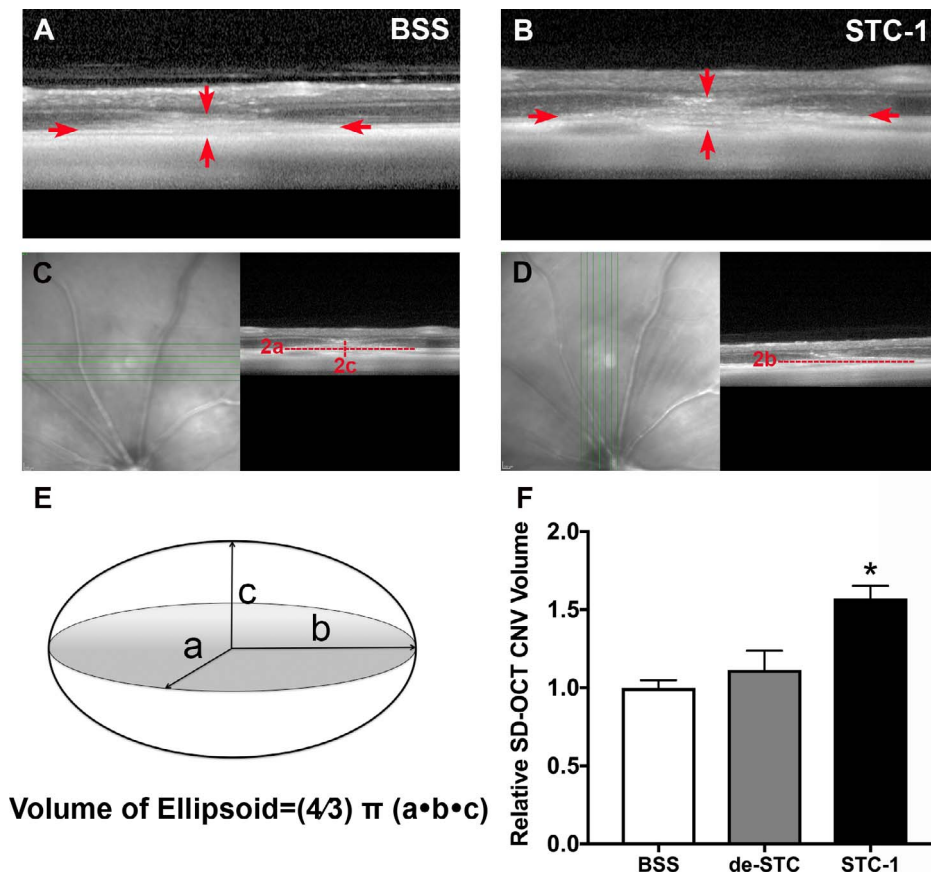
FIGURE 3. SD-OCT volume of laser-induced CNV lesions. The CNV lesion was a spindle-shaped, hyperreflective area outlined by the *red arrows*, which show the CNV lesions in the BSS control (**A**) and STC-1 treatment (**B**) groups. The width (2a), thickness (2c), and length (2b) of the CNV lesions were measured (**C**, **D**). The CNV volume was quantified based on the ellipsoid volume formula (**E**). The volume of the CNV lesions was not different between BSS ($n = 12$ animals) and de-STC-1 ($n = 3$ animals) groups, but STC-1 treatment ($n = 12$ animals) significantly increased the volume of the CNV lesion (**F**, *$P < 0.05$ vs. BSS and de-STC; 1-way ANOVA followed by Tukey's test).

appearing RPE/choroidal tissue outside the area of laser application (Fig. 5C). The expression of STC-1 was enhanced in the region of the CNV lesion compared with the surrounding RPE/choroidal tissue.

VEGF and VEGFR2 Protein Expressions

VEGF protein expression was detected in the RPE/choroidal tissue of normal eyes and its expression level was elevated in the eyes subjected to laser-induced CNV (Fig. 6A). With STC-1 treatment, the laser-induced VEGF expression was further enhanced (Fig. 6A). The VEGFR2 expression level was not significantly altered in the BSS-treated control eyes (compared with normal eyes), but was elevated in the eyes treated with STC-1 at 2 weeks after laser injury (Fig. 6B).

DISCUSSION

STC-1 was initially discovered in fish as a calcium-reducing factor.[1,2] In bony fish, STC-1 is expressed only in the corpuscles of Stannius, which are located on the ventral surface of the kidneys. Mammalian STC-1 is expressed in many different organs and is highly conserved.[3,34,35] STC-1 might be a specific molecular biomarker for occult breast cancer and an indicator of poor postoperative survival in patients with colon cancer.[9] Increased expression of STC-1 may be related to angiogenesis in colon tumors.[36,37] In the present study, we demonstrated for

the first time that RPE/choroidal tissue expresses STC-1 protein, and its level is elevated in laser-induced CNV lesions in parallel with VEGF and VEGFR2 expressions. Intravitreal administration of exogenous STC-1 elevates VEGF and VEGFR2 expressions in the choroidal tissue after laser injury and enhances CNV development. It is likely that STC-1 promotes the growth of pathologic new blood vessels in a laser-induced model of CNV through upregulation of VEGF and VEGFR2 expressions.

Although the process of pathologic growth of new blood vessels from the choroidal capillaries elicited by laser photocoagulation is different from the development of wet AMD in humans, laser-induced CNV is a well-established and widely used experimental model with clinical features resembling wet AMD.[32] Therefore, we used this thermal laser injury model to investigate the impact of STC-1 on CNV development. Because CNV formation reaches the highest level at approximately 2 weeks following laser injury,[28,38,39] as confirmed in our preliminary studies (data not shown), we collected the fundus images and experimental data at this time point.

In laser-induced retinochoroidal injury, the photoreceptors and RPE are subjected to thermal insult. FAF is a relatively new technique to evaluate RPE/photoreceptor function noninvasively. FAF signal is derived from the lipofuscin accumulation in the RPE.[40] RPE lipofuscin content may reflect the metabolic activity of photoreceptor outer segment renewal. Thus, FAF
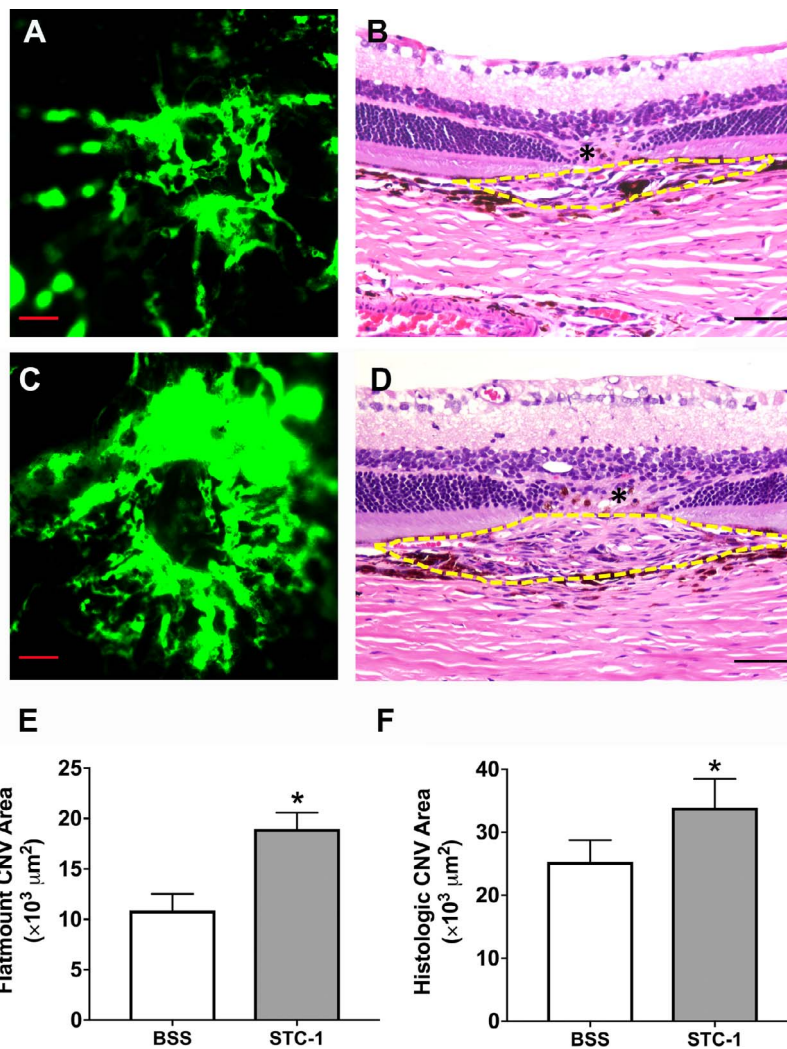
FIGURE 4. RPE-choroid-sclera flat mounts and histology of CNV lesions. Representative CNV lesions are shown in an FITC-dextran–perfused RPE-choroid-sclera flat-mount (**A**) and in histologic section (**B**) in BSS-treated eyes and in STC-1–treated eyes (**C**, **D**) 2 weeks after laser photocoagulation. Intravitreal STC-1 administration appeared to increase the area of CNV in flat mounts (**C**) and in histologic sections (**D**). Note the CNV lesion outlined with a *yellow dashed line* and the focal gliosis (*asterisk*) with pigment migration into the retina overlying the CNV lesion (**B**, **D**). See Supplementary Figure S1 for higher-magnification photomicrographs. Quantitative analysis of FITC-dextran–perfused RPE-choroid-sclera flat mounts showed a significant increase in the mean area of the CNV lesions with STC-1 ($n = 6$ animals) vs. BSS ($n = 6$ animals) treatment (**E**, *$P < 0.05$; Student's *t*-test). The mean area of the CNV lesions was significantly increased in the eyes treated with STC-1 ($n = 4$ animals) compared with BSS controls ($n = 4$ animals) as measured by histologic sections (**F**, *$P < 0.05$; Student's *t*-test).

imaging can provide useful information about the distribution of lipofuscin in the RPE and allow for visualization of the RPE-photoreceptor cell complex. Decreased FAF may indicate RPE/photoreceptor cell loss, whereas increased FAF may indicate lipofuscin release and photoreceptor inner/outer segment disruption after acute injury and retinal gliosis in healed lesions.[40–42]

In this study, FAF of CNV lesions showed a concentric, target-shaped pattern. The central, intense laser-damaged area corresponded to a small, well-circumscribed, central area of increased FAF. The central increased FAF was surrounded by a ring of decreased FAF, corresponding histologically to tissue injury with loss of the photoreceptors and RPE. In most of the CNV lesions, an additional outer ring of increased FAF was observed (Fig. 1), corresponding histologically to disorganized photoreceptors and variable attenuation and hypertrophy of the RPE. At 2 weeks after laser injury, the central increased FAF appeared to correlate histologically with focal retinal gliosis, in agreement with the reported increase in FAF with glial cell

proliferation in the retina.[42] In the eyes treated with STC-1, the intensity of FAF was significantly increased (approximately 50%) at 2 weeks after laser injury. Moreover, the area of increased FAF corresponded with the increased size of CNV as measured by SD-OCT, flat mounts, and histology in the STC-1–treated eyes, suggesting the promotion of CNV development by STC-1.

Although increased vascular leakage is commonly observed in CNV development, very limited information is available on the effect of STC-1 on vascular permeability. It has been reported that there is no difference between wild-type and STC-1$^{-/-}$ animals in blood-brain barrier (BBB) permeability under physiological or hypoxic conditions, suggesting that STC-1 does not play an important role in BBB integrity under the conditions studied.[43] On the other hand, STC-1 appears to preserve the endothelial tight junction after challenge with TNF-α in cultured human coronary artery endothelial cells.[44] In the present study, the increase in fluorescence area and intensity was used as an index for vascular leakage based on
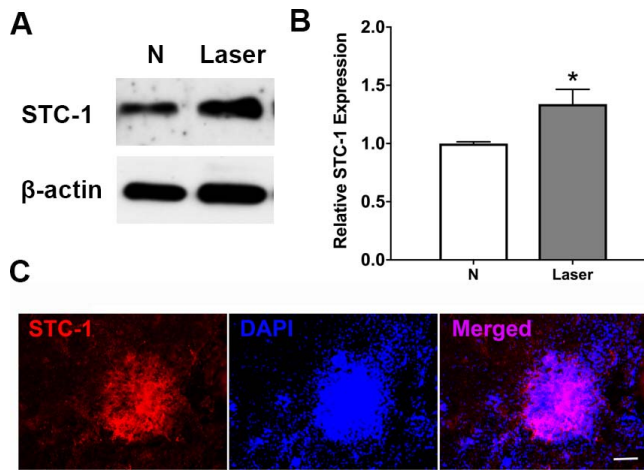
FIGURE 5. STC-1 protein detection in RPE/choroidal tissue. Western blot analysis revealed STC-1 protein expression (**A**) in normal RPE/choroidal tissue without laser treatment (N) and 2 weeks after laser treatment (Laser). STC-1 expression was significantly elevated in the RPE/choroidal tissue 2 weeks after laser injury (**B**, *$P < 0.05$ vs. N, $n = 4$ experiments; Student's *t*-test). Immunofluorescence signal of STC-1 (**C**) was detected in the CNV lesion and in normal-appearing RPE/choroidal tissue outside the area of laser application and CNV ($n = 6$ lesion sites). The expression of STC-1 was enhanced in the region of the CNV lesion compared with the surrounding RPE/choroidal tissue. Cell nuclei were stained with DAPI. *Scale bar*: 50 μm.

the grading system described previously.[31] We found that 52% of all laser-induced CNV lesions showed significant elevation of fluorescein signal (grade 3) in the eyes treated with STC-1 compared with 25% in the control eyes (Fig. 2). Intravitreal administration of STC-1 increased the severity of FFA leakage, suggesting that STC-1 might increase vascular permeability in the newly formed blood vessels and/or increase the size of neovascularization, perhaps through upregulation of VEGF protein expression, as discussed below. Interestingly, the area of increased FAF corresponded to the area of fluorescein leakage on FFA in both STC-1– and BSS-treated eyes. These data may suggest the usefulness of FAF assessment as a noninvasive method for the evaluation of CNV leakage.

In the present study, we applied three different methods to evaluate the size of CNV lesions. We used in vivo SD-OCT analysis and ex vivo measurements (FITC-perfused flat-mount preparations and histology). Each of these methods demonstrated a significant increase in the size of the CNV lesion after STC-1 treatment. Among the three different methods used, SD-OCT was the most useful tool for noninvasive longitudinal assessments of retinochoroidal structure with high resolution. However, it should be noted that the CNV volume, quantified by the ellipsoid volume formula by SD-OCT,[27] may not be accurate in this study because the CNV lesions may not have a perfect ellipsoidal shape. Nevertheless, this simple quantification method provided a reproducible and comparable evaluation for CNV lesion size that corresponded well with the results obtained from flat-mount preparations and histological studies and in accordance with other experimental models.[38,45] The high-molecular-weight FITC-dextran perfusion flat-mount technique is also a widely used method to visualize vasculature and evaluate CNV lesions. Vessels can be labeled by perfusion with high-molecular-weight FITC-dextran.[39] However, this ex vivo measurement may underestimate the volume of CNV, because it reveals only perfused choroidal vessels. Each of the three different CNV size quantification methods suggested that intravitreal STC-1 administration
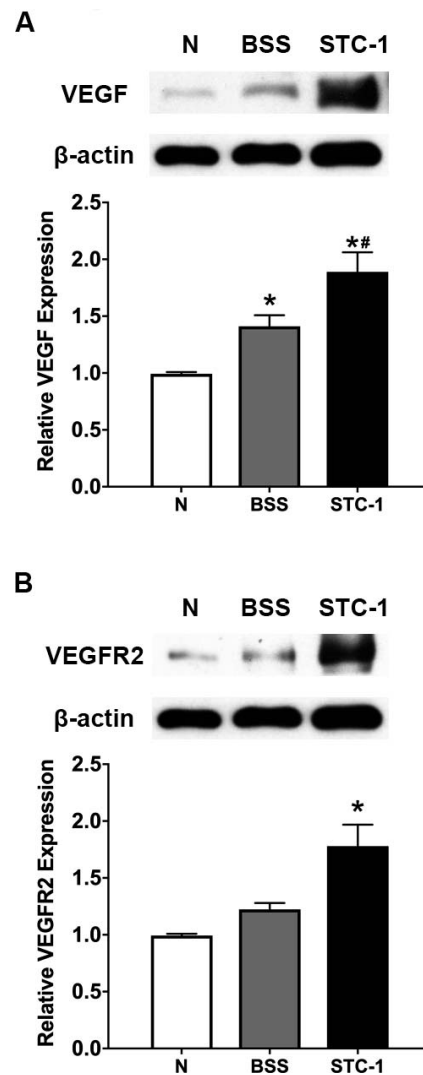
FIGURE 6. Western blot analysis of VEGF and VEGFR2 expression. VEGF protein expression (**A**) was detected in the RPE/choroidal tissue of normal eyes without laser photocoagulation (N). Quantitative analysis revealed an increase in the relative expression of VEGF in the BSS and STC-1 treated eyes with laser-induced CNV (*$P < 0.05$ vs. N, $n = 11$ experiments; 1-way ANOVA followed by Tukey's test). STC-1 treatment further increased VEGF protein expression in the RPE/choroidal tissue after laser injury (#$P < 0.05$ vs. BSS; 1-way ANOVA followed by Tukey's). VEGFR2 protein expression (**B**) was detected in the RPE/choroidal tissue of normal eyes without laser photocoagulation (N). VEGFR2 protein expression was not significantly altered by intravitreal injections of BSS. In contrast, intravitreal STC-1 administration significantly increased VEGFR2 expression (*$P < 0.05$ vs. N and BSS, $n = 5$ experiments; 1-way ANOVA followed by Tukey's test).

enhances pathological new blood vessel growth triggered by laser injury.

In the present study, we demonstrated a pro-angiogenic action of STC-1, which might also act as a pro-permeability factor to promote leakage of newly formed vasculature. This context is supported by the observed upregulation of VEGF and VEGFR2 protein expression in the choroidal tissue harvested from the eyes treated with STC-1. In this experimental model, it is speculated that intravitreal STC-1 may enhance neovascularization and promote vascular leakage via increased VEGF expression or direct activation of VEGFR2, because VEGF and its receptor signaling are known to play a

significant role in CNV formation[46] in ocular diseases related to vascular disorders, in addition to their action in enhancing vascular permeability.[47,48]

Although the exact mechanisms of CNV formation have not been fully elucidated, the imbalance of pro- and anti-angiogenic factors has been suggested to be the most important contributing factor for the initiation and promotion of neovascularization.[46–48] VEGFR2 is the main pro-angiogenic receptor expressed by endothelial cells.[49] The binding of VEGF to VEGFR2 induces receptor dimerization and auto-phosphorylation at multiple tyrosine sites for promoting cell proliferation and other biological actions.[49] Interestingly, the pro-angiogenic effect of STC-1 related to increased VEGF and phospho-VEFGR2/KDR expression has been suggested in cultured HUVECs overexpressed with STC-1.[14] Although the signaling pathway for VEGF/VEGFR2 upregulation by STC-1 remains unclear, the involvement of PKCβII and extracellular signal-regulated protein kinases 1 and 2 has been suggested in gastric cancer cells.[11] On the contrary, other studies showed the inhibition of VEGF expression by STC in ovarian granulosa cells,[50] suggesting the potential tissue- or cell-specific function of the STC protein. In the present study, we were unable to detect a significant expression of phospho-VEGFR2 due to insufficient amount of protein harvested from the RPE/choroidal tissue even though the total expression of VEGFR2 protein was augmented by STC-1. Nevertheless, the increase in STC-1 expression in the RPE/choroidal tissue subjected to laser injury and the pro-angiogenic effect of STC-1, in association with VEGF/VEGFR2 upregulation, are apparent in the promotion of laser-induced CNV formation in the present study.

Very limited information is currently available on the potential therapeutic effects of STC-1 in ocular tissues. Topical administration of STC-1 was recently demonstrated to reduce IOP in mice.[51] Interestingly, intravitreal injection of STC-1 has been shown to reduce retinal ganglion cell loss in the rat eye after optic nerve transection via inhibition of apoptosis and oxidative damage.[52] We previously reported the protective role of STC-1 in reducing photoreceptor degeneration and oxidative stress in naturally occurring (Royal College of Surgeons) and rhodopsin transgenic (S334ter-3, S334ter-4, and P23H-1) rat models of inherited retinal degeneration.[24,25] In those studies, no retinal or choroidal neovascularization was observed, and no adverse ocular effects were reported after intravitreal STC-1 administration. On the contrary, functional (ERG) and histologic rescue by STC-1 were demonstrated.[24,25] Although it remains unclear whether these beneficial effects can be observed in the present study, the anti-apoptotic or pro-survival effect of STC-1 might have contributed to the growth of CNV as a reparative process after laser injury to the retinochoroidal tissue.

In conclusion, our present study is the first to demonstrate the endogenous expression of STC-1 in choroidal tissue. The development of neovascularization and leakage following laser injury is associated with the elevation of choroidal expression of STC-1 and VEGF proteins. Administration of exogenous STC-1 enhances VEGF/VEGFR2 upregulation and promotes CNV formation after retinochoroidal laser injury. Because intravitreal STC-1 administration does not display neovascularization properties in inherited forms of retinal degeneration,[24,25] it remains unclear whether the promotion of CNV formation observed in the present study is specific to the physical injury (i.e., thermal laser photocoagulation) of the retina. Although STC-1 has been shown to protect photoreceptors from oxidative insult and enhance neural cell survival, the therapeutic potential of STC-1 in various forms of ocular disease deserves further investigation.

References

1. Lafeber FP, Hanssen RG, Choy YM, et al. Identification of hypocalcin (teleocalcin) isolated from trout Stannius corpuscles. *Gen Comp Endocrinol*. 1988;69:19–30.

2. Wagner GF, Hampong M, Park CM, Copp DH. Purification, characterization, and bioassay of teleocalcin, a glycoprotein from salmon corpuscles of Stannius. *Gen Comp Endocrinol*. 1986;63:481–491.

3. Wagner GF, Guiraudon CC, Milliken C, Copp DH. Immunological and biological evidence for a stanniocalcin-like hormone in human kidney. *Proc Natl Acad Sci U S A*. 1995; 92:1871–1875.

4. Ishibashi K, Imai M. Prospect of a stanniocalcin endocrine/paracrine system in mammals. *Am J Physiol Renal Physiol*. 2002;282:F367–F375.

5. Yeung BH, Law AY, Wong CK. Evolution and roles of stanniocalcin. *Mol Cell Endocrinol*. 2012;349:272–280.

6. Hasilo CP, McCudden CR, Gillespie JR, et al. Nuclear targeting of stanniocalcin to mammary gland alveolar cells during pregnancy and lactation. *Am J Physiol Endocrinol Metab*. 2005;289:E634–E642.

7. Filvaroff EH, Guillet S, Zlot C, et al. Stanniocalcin 1 alters muscle and bone structure and function in transgenic mice. *Endocrinology*. 2002;143:3681–3690.

8. Westberg JA, Serlachius M, Lankila P, Penkowa M, Hidalgo J, Andersson LC. Hypoxic preconditioning induces neuroprotective stanniocalcin-1 in brain via IL-6 signaling. *Stroke*. 2007; 38:1025–1030.

9. Wascher RA, Huynh KT, Giuliano AE, et al. Stanniocalcin-1: a novel molecular blood and bone marrow marker for human breast cancer. *Clin Cancer Res*. 2003;9:1427–1435.

10. Liu G, Yang G, Chang B, et al. Stanniocalcin 1 and ovarian tumorigenesis. *J Natl Cancer Inst*. 2010;102:812–827.

11. He LF, Wang TT, Gao QY, et al. Stanniocalcin-1 promotes tumor angiogenesis through up-regulation of VEGF in gastric cancer cells. *J Biomed Sci*. 2011;18:39.

12. Chakraborty A, Brooks H, Zhang P, et al. Stanniocalcin-1 regulates endothelial gene expression and modulates transendothelial migration of leukocytes. *Am J Physiol Renal Physiol*. 2007;292:F895–F904.

13. Zlot C, Ingle G, Hongo J, et al. Stanniocalcin 1 is an autocrine modulator of endothelial angiogenic responses to hepatocyte growth factor. *J Biol Chem*. 2003;278:47654–47659.

14. Law AY, Wong CK. Stanniocalcin-1 and -2 promote angiogenic sprouting in HUVECs via VEGF/VEGFR2 and angiopoietin signaling pathways. *Mol Cell Endocrinol*. 2013;374:73–81.

15. Stefansson E, Geirsdottir A, Sigurdsson H. Metabolic physiology in age related macular degeneration. *Prog Retin Eye Res*. 2011;30:72–80.

16. Jager RD, Mieler WF, Miller JW. Age-related macular degeneration. *N Engl J Med*. 2008;358:2606–2617.

17. Wankun X, Wenzhen Y, Min Z, et al. Protective effect of paeoniflorin against oxidative stress in human retinal pigment epithelium in vitro. *Mol Vis*. 2011;17:3512–3522.

18. Zhao M, Bai Y, Xie W, et al. Interleukin-1β level is increased in vitreous of patients with neovascular age-related macular

degeneration (nAMD) and polypoidal choroidal vasculopathy (PCV). *PLoS One*. 2015;10:e0125150.

19. Nowak JZ. Age-related macular degeneration (AMD): pathogenesis and therapy. *Pharmacol Rep*. 2006;58:353–363.

20. Bressler NM, Bressler SB, Fine SL. Age-related macular degeneration. *Surv Ophthalmol*. 1988;32:375–413.

21. Nita M, Grzybowski A. The role of the reactive oxygen species and oxidative stress in the pathomechanism of the age-related ocular diseases and other pathologies of the anterior and posterior eye segments in adults. *Oxid Med Cell Longev*. 2016;2016:3164734.

22. Carmeliet P, Jain RK. Angiogenesis in cancer and other diseases. *Nature*. 2000;407:249–257.

23. Yancopoulos GD, Davis S, Gale NW, Rudge JS, Wiegand SJ, Holash J. Vascular-specific growth factors and blood vessel formation. *Nature*. 2000;407:242–248.

24. Roddy GW, Rosa RH Jr, Oh JY, et al. Stanniocalcin-1 rescued photoreceptor degeneration in two rat models of inherited retinal degeneration. *Mol Ther*. 2012;20:788–797.

25. Roddy GW, Yasumura D, Matthes MT, et al. Long-term photoreceptor rescue in two rodent models of retinitis pigmentosa by adeno-associated virus delivery of Stanniocalcin-1. *Exp Eye Res*. 2017;165:175–181.

26. Gerritsen ME, Soriano R, Yang S, et al. In silico data filtering to identify new angiogenesis targets from a large in vitro gene profiling data set. *Physiol Genomics*. 2002;10:13–20.

27. Sulaiman RS, Quigley J, Qi X, et al. A simple optical coherence tomography quantification method for choroidal neovascularization. *J Ocul Pharmacol Ther*. 2015;31:447–454.

28. Cui J, Liu Y, Zhang J, Yan H. An experimental study on choroidal neovascularization induced by Krypton laser in rat model. *Photomed Laser Surg*. 2014;32:30–36.

29. Liu T, Hui L, Wang YS, et al. In-vivo investigation of laser-induced choroidal neovascularization in rat using spectral-domain optical coherence tomography (SD-OCT). *Graefes Arch Clin Exp Ophthalmol*. 2013;251:1293–1301.

30. Ozone D, Mizutani T, Nozaki M, et al. Tissue plasminogen activator as an antiangiogenic agent in experimental laser-induced choroidal neovascularization in mice. *Invest Ophthalmol Vis Sci*. 2016;57:5348–5354.

31. Guthrie MJ, Osswald CR, Valio NL, Mieler WF, Kang-Mieler JJ. Objective area measurement technique for choroidal neovascularization from fluorescein angiography. *Microvasc Res*. 2014;91:1–7.

32. Lambert V, Lecomte J, Hansen S, et al. Laser-induced choroidal neovascularization model to study age-related macular degeneration in mice. *Nat Protoc*. 2013;8:2197–2211.

33. Ivanova E, Toychiev AH, Yee CW, Sagdullaev BT. Optimized protocol for retinal wholemount preparation for imaging and immunohistochemistry. *J Vis Exp*. 2013;82:e51018.

34. Olsen HS, Cepeda MA, Zhang QQ, Rosen CA, Vozzolo BL, Wagner GF. Human stanniocalcin: a possible hormonal regulator of mineral metabolism. *Proc Natl Acad Sci U S A*. 1996;93:1792–1796.

35. Chang AC, Dunham MA, Jeffrey KJ, Reddel RR. Molecular cloning and characterization of mouse stanniocalcin cDNA. *Mol Cell Endocrinol*. 1996;124:185–187.

36. Tamura S, Oshima T, Yoshihara K, et al. Clinical significance of STC1 gene expression in patients with colorectal cancer. *Anticancer Res*. 2011;31:325–329.

37. Ieta K, Tanaka F, Yokobori T, et al. Clinicopathological significance of stanniocalcin 2 gene expression in colorectal cancer. *Int J Cancer*. 2009;125:926–931.

38. Fukuchi T, Takahashi K, Shou K, Matsumura M. Optical coherence tomography (OCT) findings in normal retina and laser-induced choroidal neovascularization in rats. *Graefes Arch Clin Exp Ophthalmol*. 2001;239:41–46.

39. Edelman JL, Castro MR. Quantitative image analysis of laser-induced choroidal neovascularization in rat. *Exp Eye Res*. 2000;71:523–533.

40. Delori FC, Dorey CK, Staurenghi G, Arend O, Goger DG, Weiter JJ. In vivo fluorescence of the ocular fundus exhibits retinal pigment epithelium lipofuscin characteristics. *Invest Ophthalmol Vis Sci*. 1995;36:718–729.

41. von Ruckmann A, Fitzke FW, Bird AC. Distribution of fundus autofluorescence with a scanning laser ophthalmoscope. *Br J Ophthalmol*. 1995;79:407–412.

42. Shields JA, Bianciotto CG, Kivela T, Shields CL. Presumed solitary circumscribed retinal astrocytic proliferation: the 2010 Jonathan W. Wirtschafter Lecture. *Arch Ophthalmol*. 2011;129:1189–1194.

43. Durukan Tolvanen A, Westberg JA, Serlachius M, et al. Stanniocalcin 1 is important for poststroke functionality, but dispensable for ischemic tolerance. *Neuroscience*. 2013;229:49–54.

44. Chen C, Jamaluddin MS, Yan S, Sheikh-Hamad D, Yao Q. Human stanniocalcin-1 blocks TNF-α-induced monolayer permeability in human coronary artery endothelial cells. *Arterioscler Thromb Vasc Biol*. 2008;28:906–912.

45. Giani A, Thanos A, Roh MI, et al. In vivo evaluation of laser-induced choroidal neovascularization using spectral-domain optical coherence tomography. *Invest Ophthalmol Vis Sci*. 2011;52:3880–3887.

46. Campochiaro PA. Retinal and choroidal neovascularization. *J Cell Physiol*. 2000;184:301–310.

47. Witmer AN, Vrensen GF, Van Noorden CJ, Schlingemann RO. Vascular endothelial growth factors and angiogenesis in eye disease. *Prog Retin Eye Res*. 2003;22:1–29.

48. Suarez S, McCollum GW, Bretz CA, Yang R, Capozzi ME, Penn JS. Modulation of VEGF-induced retinal vascular permeability by peroxisome proliferator-activated receptor-beta/delta. *Invest Ophthalmol Vis Sci*. 2014;55:8232–8240.

49. Simons M, Gordon E, Claesson-Welsh L. Mechanisms and regulation of endothelial VEGF receptor signalling. *Nat Rev Mol Cell Biol*. 2016;17:611–625.

50. Basini G, Bussolati S, Santini SE, Grasselli F. Stanniocalcin, a potential ovarian angiogenesis regulator, does not affect endothelial cell apoptosis. *Ann N Y Acad Sci*. 2009;1171:94–99.

51. Roddy GW, Viker KB, Winkler NS, et al. Stanniocalcin-1 is an ocular hypotensive agent and a downstream effector molecule that is necessary for the intraocular pressure-lowering effects of latanoprost. *Invest Ophthalmol Vis Sci*. 2017;58:2715–2724.

52. Kim SJ, Ko JH, Yun JH, et al. Stanniocalcin-1 protects retinal ganglion cells by inhibiting apoptosis and oxidative damage. *PLoS One*. 2013;8:e63749.